Reduced-Rank DOA Estimation Algorithms Based on Alternating Low-Rank Decomposition

Linzheng Qiu, Yunlong Cai, Rodrigo C. de Lamare, and Minjian Zhao

***Abstract*—In this work, we propose an alternating low-rank decomposition (ALRD) approach and novel subspace algorithms for direction-of-arrival (DOA) estimation. In the ALRD scheme, the decomposition matrix for rank reduction consists of a set of basis vectors. A low-rank auxiliary parameter vector is then employed to compute the output power spectrum. Alternating optimization strategies based on recursive least squares (RLS), denoted as ALRD-RLS and modified ALRD-RLS (MARLD-RLS), are devised to compute the basis vectors and the auxiliary parameter vector. Simulations for large sensor arrays with both uncorrelated and correlated sources are presented, showing that the proposed algorithms are superior to existing techniques.**

***Index Terms*—DOA estimation, low-rank decomposition, parameter estimation.**

I. Introduction

Array signal processing has been widely used in areas such as radar, sonar and wireless communications. Many applications related to array signal processing require the estimation of the direction-of-arrival (DOA) of the sources impinging on a sensor array [1]. Among the well-known DOA estimation schemes are the Capon method and subspace-based algorithms [2] such as Multiple-Signal Classification (MUSIC) [3] and Estimation of Signal Parameters via Rotational Invariance Techniques (ESPRIT) [4]. The Capon method calculates the output power spectrum for each scanning angle according to the constrained minimum variance (CMV) criterion. Then the estimated DOAs can be obtained by finding the peaks of the output power spectrum [5]. MUSIC, ESPRIT and their improved versions [6]–[11] estimate the DOAs by exploiting the signal and the noise subspaces of the signal correlation matrix. Due to the eigenvalue decomposition (EVD) and/or the singular-value decomposition (SVD), MUSIC and ESPRIT require a high computational cost, especially for large sensor arrays. The recently proposed subspace-based auxiliary vector (AV) [12], the conjugate gradient (CG) [13] and the joint iterative optimization (JIO) algorithms [14] employ basis vectors to build the signal subspace instead of the EVD or the SVD. However, the iterative construction of the basis vectors yields a complexity comparable to the EVD. Moreover, the AV and CG algorithms cannot provide a satisfactory performance for large sensor arrays with many sources.

The performance of direction finding algorithms depends on the data record and the array size. Resorting to larger data records leads to higher estimation performance. However, large data records are not always available in wireless environments that change rapidly. Nowadays, large sensor arrays have gained importance for applications such as radar and future communication systems. Nevertheless, direction finding for large sensor arrays is associated with high computational costs. In this regard, the development of low-complexity DOA estimation algorithms for large sensor arrays and scenarios with short data records is an important research problem.

In this paper, we present an alternating low-rank[1] decomposition (ALRD) approach for DOA estimation in large sensor arrays with a large number of sources. In the ALRD scheme, a subspace decomposition matrix which consists of a set of basis vectors and an auxiliary low-rank parameter vector are employed to compute the output power spectrum. In order to avoid matrix inversions, we develop recursive least squares (RLS) type algorithms [15] to compute the basis vectors and the auxiliary parameter vector, which reduces the computational complexity. The proposed DOA estimation algorithms are referred to as ALRD-RLS and modified ALRD-RLS (MALRD-RLS), which employs a single basis vector. Simulations show that the proposed ALRD-RLS and MALRD-RLS algorithms achieve superior performance to existing techniques for large arrays with short data records.

The paper is organized as follows. In Section II, we outline the system model and the problem of DOA estimation. The proposed ALRD scheme and algorithms are presented in Section III. In Section IV, we illustrate and discuss the simulation results. Finally, Section V concludes this work.

II. System Model and Problem Formulation

We consider a uniform linear array (ULA) with M omni-directional sensor elements and suppose that K narrowband source signals impinge on the ULA from directions θ_1, θ_2, ..., θ_K, respectively, where M is a large number with $K \ll M$. The ith snapshot of the received signal can be expressed by an $M \times 1$ vector as

$$\mathbf{r}(i) = \sum_{k=1}^{K} \mathbf{a}(\theta_k) b_k(i) + \mathbf{n}(i), \qquad (1)$$

where $b_k(i)$ is the kth source signal with power σ_b^2. The vector $\mathbf{n}(i)$ is noise vector, which is assumed to be temporally and spatially white Gaussian with zero mean and variance σ_n^2. The array steering vector $\mathbf{a}(\theta_k)$ is defined as

$$\mathbf{a}(\theta_k) = [1, e^{-2\pi j \frac{d_s}{\lambda_c} \cos\theta_k}, ..., e^{-2\pi j (M-1) \frac{d_s}{\lambda_c} \cos\theta_k}]^T, \qquad (2)$$

[1] A low-rank parameter vector arises from the solution of a low-rank system of equations. This rank also corresponds to the dimension or length of the parameter vector.

L. Qiu, Y. Cai and M. Zhao are with the Department of Information Science and Electronic Engineering, Zhejiang University, Hangzhou, China, 310027. R. C. de Lamare is with CETUC, PUC-Rio Rua Marques de So Vicente, 22493-900 Rio de Janeiro, Brazil and University of York, Heslington, YO10 5DD, York, England, United Kingdom. Email: lzqiu@zju.edu.cn, ylcai@zju.edu.cn, rcdl500@ohm.york.ac.uk, mjzhao@zju.edu.cn.

This work was supported in part by CNPq and FAPERJ, Brazil, the National Natural Science Foundation of China under Grants 61471319, Zhejiang Provincial Natural Science Foundation of China under Grant LY14F010013, the Fundamental Research Funds for the Central Universities, and the National High Technology Research and Development Program (863 Program) of China under Grant 2014AA01A707.

where $(\cdot)^T$ denotes the transpose operation and λ_c is the signal wavelength. The parameter $d_s = \frac{\lambda_c}{2}$ represents the array inter-element spacing. Direction finding algorithms aim to estimate the DOAs $\boldsymbol{\theta} = [\theta_1 \ldots \theta_K]^T$ by processing $\mathbf{r}(i)$. The correlation matrix of $\mathbf{r}(i)$ is given by

$$\mathbf{R} = \mathbb{E}\{\mathbf{r}(i)\mathbf{r}^H(i)\} = \sum_{k=1}^{K} \mathbf{a}(\theta_k)\mathbf{R}_{b,k}\mathbf{a}^H(\theta_k) + \sigma_n^2\mathbf{I}_M, \quad (3)$$

where $\mathbb{E}\{\cdot\}$ denotes expectation, $(\cdot)^H$ is the Hermitian operator and $\mathbf{I}_M$ is an identity matrix with dimension M. $\mathbf{R}_{b,k} = \mathbb{E}\{b_k(i)b_k^H(i)\}$ is the correlation matrix of the kth signal. $\mathbf{R}_n = \mathbb{E}\{\mathbf{n}(i)\mathbf{n}^H(i)\} = \sigma_n^2\mathbf{I}_M$ is the correlation matrix of the noise vector. Note that the exact knowledge of $\mathbf{R}$ is difficult to obtain, thus estimation by sample averages is employed in practice, which employs $\widehat{\mathbf{R}} = \frac{1}{N}\sum_{i=1}^{N}\mathbf{r}(i)\mathbf{r}^H(i)$, with N being the number of available snapshots.

III. Proposed ARLD Scheme ALRD-RLS and MALRD-RLS Algorithms

In this section, we detail the proposed ALRD scheme and the ALRD-RLS and MALRD-RLS DOA estimation algorithms. The ALRD scheme divides the received vector into several segments and processes each segment with an individual basis vector. The basis vectors constitute the columns of the decomposition matrix, which performs dimensionality reduction. Then, a lower dimensional data vector is processed by the auxiliary parameter vector to construct the output power spectrum. The ARLD-RLS and the MARLD-RLS algorithms are based on an alternating optimization procedure of the basis vectors and the reduced-rank auxiliary parameter vector.

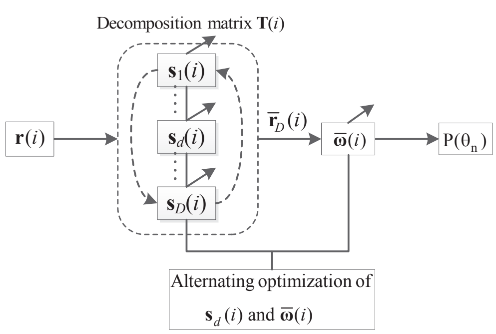

Fig. 1. Block diagram of the ALRD scheme

A. Proposed ALRD Scheme

The block diagram of the ALRD scheme is depicted in Fig. 1. The received vector $\mathbf{r}(i) = [r_0(i) \ldots r_{M-1}(i)]^T$ is processed by an $M \times D$ decomposition matrix $\mathbf{T}(i)$, which is constructed by a set of $I \times 1$ basis vectors $\mathbf{s}_d(i)$, where $d \in \{1, \ldots, D\}$. The $D \times 1$ reduced-rank data vector can be expressed by

$$\bar{\mathbf{r}}_D(i) = \mathbf{T}^H(i)\mathbf{r}(i) = \sum_{d=1}^{D}\mathbf{q}_d\mathbf{d}_d^H\boldsymbol{\mathcal{R}}(i)\mathbf{s}_d^*(i), \quad (4)$$

where $\mathbf{q}_d$ is a $D \times 1$ vector with a one in the dth position and zeros elsewhere. $\mathbf{d}_d$ is the $M \times 1$ selection vector to divide $\mathbf{r}(i)$ into D segments, which are defined as:

$$\mathbf{d}_d = [\ \underbrace{0, \ldots, 0}_{\mu_d\ zeros},\ 1\ ,\ \underbrace{0, \ldots, 0}_{M-\mu_d-1\ zeros}\ ]^T, \quad (5)$$

where μ_d is the selection pattern chosen as $\mu_d = (d-1)\lfloor \frac{M}{D} \rfloor$. Then the dth column of $\mathbf{T}(i)$ can be described as

$$\mathbf{t}_d(i) = [\ \underbrace{0, \ldots, 0}_{\mu_d\ zeros},\ \mathbf{s}_d^T(i)\ ,\ \underbrace{0, \ldots, 0}_{M-\mu_d-I\ zeros}\ ]^T. \quad (6)$$

The $M \times I$ matrix $\boldsymbol{\mathcal{R}}(i)$ with the samples of $\mathbf{r}(i)$ has a Hankel structure [16], which is described by

$$\boldsymbol{\mathcal{R}}(i) = \begin{pmatrix} r_0(i) & r_1(i) & \ldots & r_{I-1}(i) \\ \vdots & \vdots & \ldots & \vdots \\ r_{M-I}(i) & r_{M-I+1}(i) & \ldots & r_{M-1}(i) \\ r_{M-I+1}(i) & r_{M-I+2}(i) & \ldots & 0 \\ \vdots & \vdots & \ddots & \vdots \\ r_{M-1}(i) & 0 & 0 & 0 \end{pmatrix}. \quad (7)$$

After dimensionality reduction, $\bar{\mathbf{r}}_D(i)$ is processed by a $D \times 1$ auxiliary parameter vector $\bar{\boldsymbol{\omega}}(i)$ to compute the output power spectrum. As seen from Fig. 1, $\mathbf{s}_d(i)$ and $\bar{\boldsymbol{\omega}}(i)$ are alternately optimized according to a prescribed criterion, which is introduced in what follows.

B. Proposed ALRD-RLS DOA Estimation Algorithm

The ALRD-RLS algorithm based on the CMV criterion solves the optimization problem:

$$\begin{aligned} &\min_{\bar{\boldsymbol{\omega}}(i),\mathbf{s}_d(i)} \sum_{l=1}^{i}\alpha^{i-l}\Big|\bar{\boldsymbol{\omega}}^H(i)\sum_{d=1}^{D}\mathbf{q}_d\mathbf{d}_d^H\boldsymbol{\mathcal{R}}(l)\mathbf{s}_d^*(i)\Big|^2 \\ &\text{subject to} \quad \bar{\boldsymbol{\omega}}^H(i)\sum_{d=1}^{D}\mathbf{q}_d\mathbf{d}_d^H\boldsymbol{\mathcal{A}}_n\mathbf{s}_d^*(i) = 1 \end{aligned}, \quad (8)$$

where α is a forgetting factor close to but smaller than 1 [15]. $\boldsymbol{\mathcal{A}}_n$ is the $M \times I$ Hankel matrix of the scanning steering vector $\mathbf{a}(\theta_n) = [a_0(\theta_n) \ldots a_{M-1}(\theta_n)]^T$, which is given by

$$\boldsymbol{\mathcal{A}}_n(i) = \begin{pmatrix} a_0(\theta_n) & a_1(\theta_n) & \ldots & a_{I-1}(\theta_n) \\ \vdots & \vdots & \ldots & \vdots \\ a_{M-I}(\theta_n) & a_{M-I+1}(\theta_n) & \ldots & a_{M-1}(\theta_n) \\ a_{M-I+1}(\theta_n) & a_{M-I+2}(\theta_n) & \ldots & 0 \\ \vdots & \vdots & \ddots & \vdots \\ a_{M-1}(\theta_n) & 0 & 0 & 0 \end{pmatrix}. \quad (9)$$

The optimization problem in (8) can be solved by the method of Lagrange multipliers whose Lagrangian is described by

$$\begin{aligned} \mathcal{L}(i) = &\sum_{l=1}^{i}\alpha^{i-l}\Big|\bar{\boldsymbol{\omega}}^H(i)\sum_{d=1}^{D}\mathbf{q}_d\mathbf{d}_d^H\boldsymbol{\mathcal{R}}(l)\mathbf{s}_d^*(i)\Big|^2 \\ &+ 2\Re\{\lambda[\bar{\boldsymbol{\omega}}^H(i)\sum_{d=1}^{D}\mathbf{q}_d\mathbf{d}_d^H\boldsymbol{\mathcal{A}}_n\mathbf{s}_d^*(i) - 1]\}, \end{aligned} \quad (10)$$

where $\Re\{\cdot\}$ selects the real part of the argument. By taking the gradient of (10) with respect to $\mathbf{s}_d(i)$, we obtain

$$\begin{aligned} \frac{\partial\mathcal{L}(i)}{\partial\mathbf{s}_d(i)} = &\sum_{l=1}^{i}\alpha^{i-l}\boldsymbol{\mathcal{R}}^H(l)\mathbf{d}_d\mathbf{q}_d^H\bar{\boldsymbol{\omega}}(i)\bar{\boldsymbol{\omega}}^H(i)\mathbf{q}_d\mathbf{d}_d^H\boldsymbol{\mathcal{R}}(l)\mathbf{s}_d^*(i) \\ &+ \sum_{l=1}^{i}\alpha^{i-l}\boldsymbol{\mathcal{R}}^H(l)\mathbf{d}_d\mathbf{q}_d^H\bar{\boldsymbol{\omega}}(i)\bar{\boldsymbol{\omega}}^H(i)\sum_{j\neq d}^{D}\mathbf{q}_j\mathbf{d}_j^H\boldsymbol{\mathcal{R}}(l)\mathbf{s}_j^*(i) \\ &+ \lambda^*\boldsymbol{\mathcal{A}}_n^H\mathbf{d}_d\mathbf{q}_d^H\bar{\boldsymbol{\omega}}(i). \end{aligned} \quad (11)$$

By equating (11) to zero and solving for $\mathbf{s}_d(i)$, we have

$$\mathbf{s}_d(i) = -\mathbf{R}_{s,d}^{-1}(i)\sum_{j\neq d}^{D}\mathbf{P}_{s,j}(i) - \lambda\mathbf{R}_{s,d}^{-1}(i)\boldsymbol{\mathcal{A}}_n^T\mathbf{d}_d\mathbf{q}_d^H\bar{\boldsymbol{\omega}}^*(i). \quad (12)$$

where

$$\mathbf{R}_{s,d}(i)=\sum_{l=1}^{i}\alpha^{i-l}\boldsymbol{\mathcal{R}}^T(l)\mathbf{d}_d\mathbf{q}_d^H\bar{\boldsymbol{\omega}}^*(i)\bar{\boldsymbol{\omega}}^T(i)\mathbf{q}_d\mathbf{d}_d^H\boldsymbol{\mathcal{R}}^*(l), \tag{13}$$

$$\mathbf{P}_{s,j}(i)=\sum_{l=1}^{i}\alpha^{i-l}\boldsymbol{\mathcal{R}}^T(l)\mathbf{d}_d\mathbf{q}_d^H\bar{\boldsymbol{\omega}}^*(i)\bar{\boldsymbol{\omega}}^T(i)\mathbf{q}_j\mathbf{d}_j^H\boldsymbol{\mathcal{R}}^*(l)\mathbf{s}_j(i). \tag{14}$$

Substituting (12) into (8), we obtain the Lagrange multiplier:

$$\lambda=\frac{\sum\limits_{j\neq d}^{D}\mathbf{q}_j^H\bar{\boldsymbol{\omega}}(i)\mathbf{d}_d^H\boldsymbol{\mathcal{A}}_n^*\mathbf{s}_j(i-1)-1-\prod(i)\mathbf{R}_{s,d}^{-1}(i)\sum\limits_{j\neq d}^{D}\mathbf{P}_{s,j}(i)}{\prod(i)\mathbf{R}_{s,d}^{-1}(i)\prod^H(i)}, \tag{15}$$

where $\prod(i)=\mathbf{q}_d^H\bar{\boldsymbol{\omega}}(i)\mathbf{d}_d^H\boldsymbol{\mathcal{A}}_n^*$. Based on (12) and (15), we obtain the dth basis vector $\mathbf{s}_d(i)$.

Next we consider the update of $\mathbf{R}_{s,d}^{-1}(i)$. By applying the matrix inversion lemma [15] to (13), we obtain

$$\mathbf{g}_{s,d}(i)=\frac{\mathbf{R}_{s,d}^{-1}(i-1)\boldsymbol{\mathcal{R}}^T(i)\mathbf{d}_d}{\alpha\beta+\mathbf{d}_d^H\boldsymbol{\mathcal{R}}^*(i)\mathbf{R}_{s,d}^{-1}(i-1)\boldsymbol{\mathcal{R}}^T(i)\mathbf{d}_d}, \tag{16}$$

$$\mathbf{R}_{s,d}^{-1}(i)=\alpha^{-1}\mathbf{R}_{s,d}^{-1}(i-1)-\alpha^{-1}\mathbf{g}_{s,d}(i)\mathbf{d}_d^H\boldsymbol{\mathcal{R}}^*(i)\mathbf{R}_{s,d}^{-1}(i-1), \tag{17}$$

where $\beta=(\mathbf{q}_d^H\bar{\boldsymbol{\omega}}^*(i)\bar{\boldsymbol{\omega}}^T(i)\mathbf{q}_d)^{-1}$. As with $\mathbf{P}_{s,j}(i)$, we obtain it through iterations:

$$\mathbf{P}_{s,j}(i)=\alpha\mathbf{P}_{s,j}(i-1)+\boldsymbol{\mathcal{R}}^T(i)\mathbf{d}_d\mathbf{q}_d^H\bar{\boldsymbol{\omega}}^*(i)\bar{\boldsymbol{\omega}}^T(i)\mathbf{q}_j\mathbf{d}_j^H\boldsymbol{\mathcal{R}}^*(i)\mathbf{s}_j(i). \tag{18}$$

By employing (12)-(18), we can update $\mathbf{s}_d(i)$ for $d\in\{1,\ldots,D\}$. Given the values of $\mathbf{s}_d(i)$, we can compute $\bar{\boldsymbol{\omega}}(i)$. Defining $\bar{\mathbf{a}}(i)=\sum_{d=1}^{D}\mathbf{q}_d\mathbf{d}_d^H\boldsymbol{\mathcal{A}}_n\mathbf{s}_d^*(i)$ and $\bar{\mathbf{r}}_D(l)=\sum_{d=1}^{D}\mathbf{q}_d\mathbf{d}_d^H\boldsymbol{\mathcal{R}}(l)\mathbf{s}_d^*(i)$, (8) can be modified as

$$\min_{\bar{\boldsymbol{\omega}}(i)}\quad\sum_{l=1}^{i}\alpha^{i-l}\left|\bar{\boldsymbol{\omega}}^H(i)\bar{\mathbf{r}}_D(l)\right|^2\quad\text{subject to}\quad\bar{\boldsymbol{\omega}}^H(i)\bar{\mathbf{a}}(i)=1. \tag{19}$$

Solving for $\bar{\boldsymbol{\omega}}(i)$, we have

$$\boldsymbol{g}_D(i)=\frac{\mathbf{R}_D^{-1}(i-1)\bar{\mathbf{r}}_D(i)}{\alpha+\bar{\mathbf{r}}_D^H(i)\mathbf{R}_D^{-1}(i-1)\bar{\mathbf{r}}_D(i)}, \tag{20}$$

$$\mathbf{R}_D^{-1}(i)=\alpha^{-1}\mathbf{R}_D^{-1}(i-1)-\alpha^{-1}\boldsymbol{g}_D(i)\bar{\mathbf{r}}_D^H(i)\mathbf{R}_D^{-1}(i-1), \tag{21}$$

$$\bar{\boldsymbol{\omega}}(i)=\frac{\mathbf{R}_D^{-1}(i)\bar{\mathbf{a}}(i)}{\bar{\mathbf{a}}^H(i)\mathbf{R}_D^{-1}(i)\bar{\mathbf{a}}(i)}, \tag{22}$$

where $\mathbf{R}_D^{-1}(i)=\sum_{l=1}^{i}\alpha^{i-l}\bar{\mathbf{r}}_D(l)\bar{\mathbf{r}}_D^H(l)$. Based on the previous derivations, we calculate the output power for each scanning angle θ_n:

$$P(\theta_n)=\sum_{l=1}^{i}\alpha^{i-l}\left|\bar{\boldsymbol{\omega}}^H(i)\bar{\mathbf{r}}_D(l)\right|^2=\frac{1}{\bar{\mathbf{a}}^H(i)\mathbf{R}_D^{-1}(i)\bar{\mathbf{a}}(i)}. \tag{23}$$

By selecting the peaks of the output power spectrum, we can obtain the estimated values of the DOAs. The ALRD-RLS algorithm is summarized in Table I.

C. Proposed MALRD-RLS DOA Estimation Algorithm

By examining the structure of the ALRD scheme, we can reduce its computational cost by using a single basis vector in the decomposition matrix. From this observation, we devise a modified version of the ALRD-RLS algorithm, i.e., the MALRD-RLS algorithm. Specifically, the columns of the decomposition matrix $\mathbf{T}(i)$ in the MALRD-RLS algorithm are formed by the same basis vector $\mathbf{s}(i)$, i.e., $\mathbf{t}_d(i)=[\underbrace{0,\ldots,0}_{\mu_d\ zeros},\ \mathbf{s}^T(i)\ ,\ \underbrace{0,\ldots,0}_{M-\mu_d-I\ zeros}\ ]^T$. Subsequently, $\bar{\mathbf{r}}_D(i)=\mathbf{Q}\boldsymbol{\mathcal{R}}(i)\mathbf{s}^*(i)$, where $\mathbf{Q}=\sum_{d=1}^{D}\mathbf{q}_d\mathbf{d}_d^H$. Therefore, the optimization problem solved by the MALRD-RLS algorithm is given by

$$\min_{\bar{\boldsymbol{\omega}}(i),\mathbf{s}(i)}\quad\sum_{l=1}^{i}\alpha^{i-l}\left|\bar{\boldsymbol{\omega}}^H(i)\mathbf{Q}\boldsymbol{\mathcal{R}}(l)\mathbf{s}^*(i)\right|^2.\quad\text{subject to}\quad\bar{\boldsymbol{\omega}}^H(i)\mathbf{Q}\boldsymbol{\mathcal{A}}_n\mathbf{s}^*(i)=1 \tag{24}$$

This problem can be solved by following the same procedure as in the ALRD-RLS algorithm. Firstly, we construct the Lagrangian function as

$$\mathcal{L}(i)=\sum_{l=1}^{i}\alpha^{i-l}\left|\bar{\boldsymbol{\omega}}^H(i)\mathbf{Q}\boldsymbol{\mathcal{R}}(l)\mathbf{s}^*(i)\right|^2.+2\Re\{\lambda[\bar{\boldsymbol{\omega}}^H(i)\mathbf{Q}\boldsymbol{\mathcal{A}}_n\mathbf{s}^*(i)-1]\} \tag{25}$$

Secondly, we take the gradient of (25) with respect to $\mathbf{s}(i)$, set the result to zero and solve for $\mathbf{s}(i)$. The update equation of $\mathbf{s}(i)$ is given by

$$\mathbf{s}(i)=\frac{\mathbf{R}_s^{-1}(i)\boldsymbol{\mathcal{A}}_n^T\mathbf{Q}^T\bar{\boldsymbol{\omega}}^*(i)}{\bar{\boldsymbol{\omega}}^T(i)\mathbf{Q}\boldsymbol{\mathcal{A}}_n^*\mathbf{R}_s^{-1}(i)\boldsymbol{\mathcal{A}}_n^T\mathbf{Q}^T\bar{\boldsymbol{\omega}}^*(i)}, \tag{26}$$

where $\mathbf{R}_s(i)=\sum_{l=1}^{i}\alpha^{i-l}\boldsymbol{\mathcal{R}}^T(l)\mathbf{Q}^T\bar{\boldsymbol{\omega}}^*(i)\bar{\boldsymbol{\omega}}^T(i)\mathbf{Q}\boldsymbol{\mathcal{R}}^*(l)$. The matrix $\mathbf{R}_s^{-1}(i)$ can be computed as:

$$\mathbf{g}_s(i)=\frac{\mathbf{R}_s^{-1}(i-1)\boldsymbol{\mathcal{R}}^T(i)\mathbf{Q}^T\bar{\boldsymbol{\omega}}^*(i)}{\alpha+\bar{\boldsymbol{\omega}}^T(i)\mathbf{Q}\boldsymbol{\mathcal{R}}^*(i)\mathbf{R}_s^{-1}(i-1)\boldsymbol{\mathcal{R}}^T(i)\mathbf{Q}^T\bar{\boldsymbol{\omega}}^*(i)}, \tag{27}$$

$$\mathbf{R}_s^{-1}(i)=\alpha^{-1}\mathbf{R}_s^{-1}(i-1)-\alpha^{-1}\mathbf{g}_s(i)\bar{\boldsymbol{\omega}}^T(i)\mathbf{Q}\boldsymbol{\mathcal{R}}^*(i)\mathbf{R}_s^{-1}(i-1). \tag{28}$$

Next, we discuss the update of $\bar{\boldsymbol{\omega}}(i)$. By redefining $\bar{\mathbf{a}}(i)=\mathbf{Q}\boldsymbol{\mathcal{A}}_n\mathbf{s}^*(i)$, the cost function for the update of $\bar{\boldsymbol{\omega}}(i)$ is the same as that in (19). Hence $\bar{\boldsymbol{\omega}}(i)$ can also be constructed by (20)-(22) in the MALRD-RLS algorithm.

TABLE I
THE ALRD-RLS DOA ESTIMATION ALGORITHM.

1	Set N and α
2	**For** each scanning angle θ_n **do**
3	Initialize $\mathbf{R}_{s,d}^{-1}(0)$, $\mathbf{P}_{s,j}(0)$, $\mathbf{s}_d(0)$, $\bar{\boldsymbol{\omega}}(0)$
4	**For** each snapshot i ($i=1,\ldots,N$) **do**
5	**For** each basis d ($d=1,\ldots,D$) **do**
6	Update $\mathbf{s}_d(i)$ based on (12)-(18)
7	Update $\bar{\boldsymbol{\omega}}(i)$ based on (20)-(22)
8	Calculate the output power $P(\theta_n)=(\bar{\mathbf{a}}^H(N)\mathbf{R}_D^{-1}(N)\bar{\mathbf{a}}(N))^{-1}$
9	Estimate the DOA $\hat{\boldsymbol{\theta}}=\arg\ \max_{\theta_n}\ P(\theta_n)$

TABLE II
THE MALRD-RLS DOA ESTIMATION ALGORITHM.

1	Set N and α
2	**For** each scanning angle θ_n **do**
3	Initialize $\mathbf{R}_s^{-1}(0)$, $\mathbf{s}(0)$, $\bar{\boldsymbol{\omega}}(0)$
4	**For** each snapshot i ($i=1,\ldots,N$) **do**
5	Update $\mathbf{s}(i)$ based on (26)-(28)
6	Redefine $\bar{\mathbf{a}}(i)=\mathbf{Q}\boldsymbol{\mathcal{A}}_n\mathbf{s}^*(i)$ and update $\bar{\boldsymbol{\omega}}(i)$ based on (20)-(22)
7	Calculate the output power $P(\theta_n)=(\bar{\mathbf{a}}^H(N)\mathbf{R}_D^{-1}(N)\bar{\mathbf{a}}(N))^{-1}$
8	Estimate the DOA $\hat{\boldsymbol{\theta}}=\arg\ \max_{\theta_n}\ P(\theta_n)$

After the update of $\mathbf{s}(i)$ and $\bar{\boldsymbol{\omega}}(i)$, we calculate the output power spectrum based on (23). The peaks of the power spectrum are the estimated DOAs. A brief summary of the MALRD-RLS algorithm is illustrated in Table II.

D. Computational Complexity

Here we detail the computational complexity of the proposed ALRD-RLS and MALRD-RLS algorithms and several existing DOA estimation algorithms. ESPRIT uses an EVD of $\mathbf{R}$, which has complexity of $O(M^3)$. MUSIC employs both the EVD and grid search, resulting in a cost of $O(M^3 + (180/\triangle)M^2)$, with $\triangle$ being the search step. Matrix inversions and grid searches are essential for Capon, whose complexity is $O(M^3+(180/\triangle)M^2)$. For the AV and CG algorithms, the construction of the basis vectors leads to a complexity which is higher than that of the ESPRIT algorithm [12] [13]. The JIO-RLS algorithm has a cost of $O((180/\triangle)N(M^2+D^2))$, with D being the length of the reduced-rank received vector. ALRD-RLS avoids the EVD, the matrix inversion and the construction of the transformation matrix, and the update of D basis vectors and an auxiliary parameter vector requires $O((180/\triangle)N(DI^2+D^2))$. MALRD-RLS only uses one basis vector and costs $O((180/\triangle)N(I^2+D^2))$. The computational complexity of the analyzed algorithms is depicted in Table III. Even in a large sensor array, I and D are small numbers, with $I \ll M$ and $D \ll M$, the cost of ALRD-RLS and MALRD-RLS can be less than those of the existing algorithms.

TABLE III
COMPARISON OF COMPUTATIONAL COMPLEXITY.

Algorithm	Complexity
ESPRIT [4]	$O(M^3)$
MUSIC [3]	$O(M^3+(180/\triangle)M^2)$
Capon [5]	$O(M^3+(180/\triangle)M^2)$
AV [12]	$O((180/\triangle)KM^2)$
CG [13]	$O((180/\triangle)KM^2)$
JIO-RLS [14]	$O((180/\triangle)N(M^2+D^2))$
ALRD-RLS	$O((180/\triangle)N(DI^2+D^2))$
MALRD-RLS	$O((180/\triangle)N(I^2+D^2))$

IV. Simulations

In this section, we evaluate the ALRD-RLS and MALRD-RLS algorithms through simulations. A ULA with $M = 60$ elements is adopted in the experiments. $K = 15$ narrowband source signals impinge on the ULA from directions θ_k, $k \in \{1, \cdots, K\}$, with 2 of them being correlated and the others uncorrelated. The separation between θ_k and θ_{k+1} is assumed to be 3^o. The correlated sources are generated as follows:

$$b_1 \sim \mathcal{N}(0, \sigma_b^2) \quad \text{and} \quad b_2(i) = \varrho b_1(i) + \sqrt{1-\varrho^2}e(i), \quad (29)$$

where $e \sim \mathcal{N}(0, \sigma_b^2)$. ϱ is the correlation coefficient fixed as 0.7 in this work. We assume that a small number of snapshots are available and set $N = 20$ in the simulations. The source signals are modulated by a binary phase shift keying (BPSK) scheme, 13 out of 15 sources have powers $\sigma_b^2 = 1$, one with power $\sigma_b^2 = 2$, another with power $\sigma_b^2 = 4$. The search step is chosen as 0.3° for the algorithms based on grid search. In each experiment, $L = 100$ independent Monte Carlo runs are conducted to obtain the curves.

In the first experiment we assess the effects of D and I in terms of root mean square error (RMSE) performance of the proposed algorithms, which is calculated as $RMSE = \sqrt{\frac{1}{LK}\sum_{l=1}^{L}\sum_{k=1}^{K}(\hat{\theta}_{k,l} - \theta_{k,l})^2}$. We investigate the RMSE of the ALRD-RLS and MALRD-RLS algorithms with an input signal-to-noise ratio (SNR) of 5dB. Simulation result in Fig. 2 shows that the performance gets better for both the ALRD-RLS and MALRD-RLS algorithms as D and I become larger. Nevertheless, when D is greater than 7, the performance gain becomes negligible, especially for MALRD-RLS. Considering that larger D and I lead to a higher computational cost, we choose $I = 12$, $D = 5$ for both algorithms to achieve an attractive tradeoff between performance and complexity.

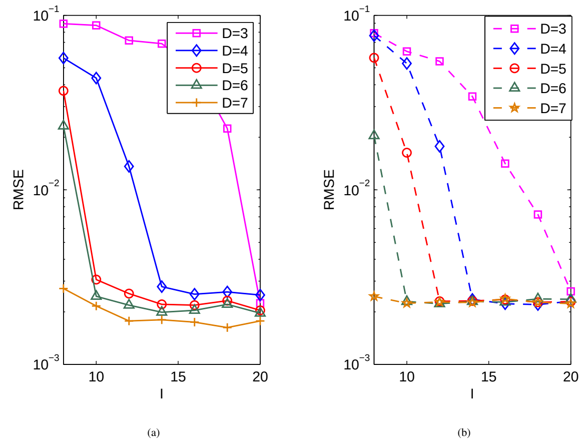

Fig. 2. RMSE versus I for different Ds for proposed algorithms. (a) ALRD-RLS (b) MALRD-RLS

We then evaluate the RMSE performance of the analyzed algorithms. We compare ALRD-RLS and MALRD-RLS with MUSIC, ESPRIT, Capon, CG, AV and the JIO-RLS algorithms. We set the parameters for JIO-RLS to $D = 5$ and $\alpha = 0.998$. For MALRD-RLS and ALRD-RLS, we choose $I = 12$, $D = 5$, $\alpha = 0.998$. From Fig. 3, MALRD-RLS provides a superior RMSE performance with the lowest threshold SNR and the lowest RMSE level in high SNRs, followed by ALRD-RLS, MUSIC, JIO-RLS, Capon and ESPRIT. The AV and CG algorithms present poor performance for large-scale sensor arrays. Note that MUSIC, ESPRIT, Capon, AV and CG require forward backward averaging (FBA) [17], [18] to ensure satisfactory performance for correlated signals.

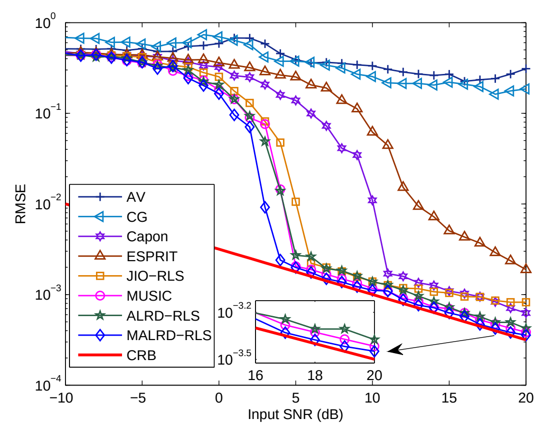

Fig. 3. RMSE versus input SNR.

V. Conclusion

In this paper, we have proposed the ALRD scheme and the ALRD-RLS and MALRD-RLS subspace DOA estimation algorithms based on alternating optimization. The proposed algorithms are suitable for large sensor arrays and have a lower computational cost than existing techniques. Simulation results show that MALRD-RLS and ALRD-RLS outperform previously reported algorithms.

REFERENCES

[1] H. Krim and M. Viberg, "Two decades of array signal processing research: the parametric approach," *IEEE Signal Processing Magazine*, vol. 13, no. 4, pp. 67–94, July 1996.

[2] H. L. V. Trees, *Optimum Array Processing: Part IV of Detection, Estimation and Modulation Theory*. John Wiley & Sons, 2002.

[3] R. O. Schmidt, "Multiple emitter location and signal parameter estimation," *IEEE Transactions on Antennas and Propagation*, vol. 34, no. 3, pp. 276–280, March 1986.

[4] R. Roy and T. Kailath, "ESPRIT-estimation of signal parameters via rotational invariance techniques," *IEEE Transactions on Acoustics, Speech and Signal Processing*, vol. 37, no. 7, pp. 984–995, Jul. 1989.

[5] J. Capon, "High-resolution frequency-wavenumber spectrum analysis," *Proceedings of the IEEE*, vol. 57, no. 8, pp. 1408–1418, Aug. 1969.

[6] K. C. Huarng and C. C. Yeh, "A unitary transformation method for angle-of-arrival estimation," *IEEE Transactions on Signal Processing*, vol. 39, no. 4, pp. 975–977, April 1991.

[7] F. G. Yan, M. Jin, and X. Qiao, "Low-complexity DOA estimation based on compressed MUSIC and its performance analysis," *IEEE Transactions on Signal Processing*, vol. 61, no. 8, pp. 1915–1930, April 2013.

[8] C. Qian, L. Huang, and H. C. So, "Improved unitary Root-MUSIC for DOA estimation based on pseudo-noise resampling," *IEEE Signal Processing Letters*, vol. 21, no. 2, pp. 140–144, February 2014.

[9] X. Mestre and M. A. Lagunas, "Modified subspace algorithms for doa estimation with large arrays," *IEEE Transactions on Signal Processing*, vol. 56, no. 2, pp. 598–614, February 2008.

[10] F. Gao and A. B. Gershman, "A generalized ESPRIT approach to direction-of-arrival estimation," *IEEE Signal Processing Letters*, vol. 12, no. 3, pp. 254–257, March 2005.

[11] N. Tayem and H. M. Kwon, "Conjugate ESPRIT (C-SPRIT)," *IEEE Transactions on Antennas and Propagation*, vol. 52, no. 10, pp. 2618–2624, Oct. 2004.

[12] R. Grover, D. A. Pados, and M. J. Medley, "Subspace direction finding with an auxiliary-vector basis," *IEEE Transactions on Signal Processing*, vol. 55, no. 2, pp. 758–763, January 2007.

[13] H. Semira and H. Belkacemi and S. Marcos, "High Resolution Source Localization Algorithm Based on the Conjugate Gradients," *EURASIP Journal on Advances in Signal Processing*, vol. 2007, pp. 1–9, March 2007.

[14] L. Wang, R. C. de Lamare, and M. Haardt, "Direction finding algorithms based on joint iterative subspace optimization," *IEEE Transactions on Aerospace and Electronic Systems*, vol. 50, no. 4, pp. 2541–2553, Oct. 2014.

[15] S. Haykin, *Adaptive Filter Theory*. Englewood Cliffs, NJ: Prentice Hall, 2002.

[16] G. H. Golub and C. F. van Loan, *Matrix Computations*. New York: Wiley, 2002.

[17] S. U. Pillai and B. H. Kwon, "Forward/backward spatial smoothing techniques for coherent signal identification," *IEEE Transactions on Acoustics, Speech and Signal Processing*, vol. 37, no. 1, pp. 8–15, January 1989.

[18] D. A. Linebarger, R. D. DeGroat, and E. M. Dowling, "Efficient direction-finding methods employing forward/backward averaging," *IEEE Transactions on Signal Processing*, vol. 42, no. 8, pp. 2136–2145, August 1994.